

The Black Death Anomaly: A Non-Abelian Field Theory of Epidemiological Safe Zones

José de Jesús Bernal-Alvarado*

Physics Engineering Department, Universidad de Guanajuato, México

David Delepine†

Physics Department, Universidad de Guanajuato, México

(Dated: March 11, 2026)

Classical reaction-diffusion models of the 14th-century Black Death fail to explain the rapid genetic radiation of *Yersinia pestis* and the anomalous emergence of vast, untouched geographic safe zones, such as Central Europe. In this work, we resolve these historical anomalies by embedding macroscopic pathogen dynamics within a non-Abelian gauge theory. Utilizing the Doi-Peliti formalism, we map the stochastic master equation of a multi-strain epidemic into a covariant classical field theory. We introduce an $SU(N)$ environmental gauge field, \mathbf{A}_μ , which actively couples geographic displacement to phenotypic mutation, treating evolutionary drift as a spatial transport phenomenon. We demonstrate via linear stability analysis that this covariant advection drives a Differential Flow (Turing-Hopf) instability, spontaneously breaking spatial symmetry to generate traveling waves of mutation. Furthermore, by extending the pathogen multiplet to the large- N ('t Hooft) continuum limit, we prove that historical safe zones are not statistical outliers nor the result of perfect quarantine, but are mathematically necessary topological voids. In this continuous limit, the destructive interference of the mutating wavefronts analytically resolves into a stable, isotropic macroscopic node governed by a zeroth-order Bessel function (J_0), precisely mapping onto the historical survival of Poland and Bohemia.

I. INTRODUCTION

Classical reaction-diffusion models of historical pandemics, such as the 14th-century Black Death, typically treat the outbreak as a homogeneous, isotropic wave of a single pathogen sweeping across a continent[1, 2]. However, this standard paradigm struggles to physically reconcile two major historical anomalies: the rapid genetic radiation of the pathogen across diverse ecological landscapes [3, 4], and the emergence of vast, abruptly untouched geographic “safe zones”—most notably the interior of Poland and Bohemia—surrounded by regions of total demographic collapse [5]. Conventional epidemiological literature often forces these safe zones into models by imposing arbitrary, static geographic boundaries or assuming absolute quarantine efficacy.

In this work, we present a unified statistical field theory model that resolves these anomalies, without relying on ad-hoc boundary conditions. By applying the Doi-Peliti formalism[6–9], the stochastic master equation of a mutating pathogen are mapped into an imaginary-time Schrödinger equation, upgrading the pathogen field to an $SU(N)$ multiplet. We introduce a non-Abelian environmental gauge field, \mathbf{A}_μ , which couples geographic displacement directly to phenotypic mutation. Through a saddle-point approximation and linear stability analysis, we demonstrate that this gauge field drives a Differential Flow (Turing-Hopf) instability [10], spontaneously generating traveling waves of mutation. Finally, by extending the model to the large- N 't Hooft continuum limit [11], we prove that historical safe zones are not statistical outliers, but topological nodes of destructive interference governed by a zeroth-order Bessel function.

The remainder of this paper is organized as follows. Section II establishes the theoretical framework, mapping the stochastic master equation into a non-Abelian gauge theory using the Doi formalism. In Section III, we derive the macroscopic mean-field equations via the saddle-point approximation, isolating the covariant advection. Section IV presents the linear stability analysis, proving the mathematical conditions required for the gauge-driven Turing-Hopf instability. Section V extends this model to a two-dimensional domain, providing numerical evidence for the spontaneous emergence of topological safe zones. In Section VI, we apply this model phenomenologically to the anomalies of the 14th-century Black Death. Finally, Section VII offers concluding remarks.

*Electronic address: bernal@ugto.mx

†Electronic address: delepine@ugto.mx

II. THEORETICAL FRAMEWORK

In the Doi formalism [6–9], the classical stochastic master equation describing the probability distribution of population numbers are mapped into an imaginary-time Schrödinger equation. Let the system contain a scalar Susceptible population S and an Infected population with N distinct, building upon field-theoretic contagion model given in [12], mutating strains, represented as an $SU(N)$ multiplet $\mathbf{I} = (I_1, I_2, \dots, I_N)^T$. The promotion of the pathogen field to an $SU(N)$ multiplet is physically mandated by the conservation of total pathogen probability amplitude during neutral mutational drift. Unlike arbitrary Markovian transition matrices used in standard multi-strain ODEs, the special unitary group $SU(N)$ describes continuous, mass-conserving rotations within the internal strain space. When an ancestral strain radiates into N distinct phenotypic lineages, the traceless Hermitian generators T^a ensure that the spontaneous conversion between strains via environmental forcing (\mathbf{A}_μ) strictly preserves the local pathogen density prior to host interaction. This symmetry enforces that spatial mutation operates as a zero-sum rotational phase shift among competing variants.

We introduce bosonic creation and annihilation operators satisfying the canonical commutation relations:

$$[a_S(\mathbf{x}), a_S^\dagger(\mathbf{y})] = \delta(\mathbf{x} - \mathbf{y}) \quad (1)$$

$$[a_{I,i}(\mathbf{x}), a_{I,j}^\dagger(\mathbf{y})] = \delta_{ij} \delta(\mathbf{x} - \mathbf{y}) \quad (2)$$

The state of the system is described by a ket $|\mathcal{P}(t)\rangle$. Its time evolution is governed by the Liouvillian operator \mathcal{L} :

$$\partial_t |\mathcal{P}(t)\rangle = -\mathcal{L} |\mathcal{P}(t)\rangle \quad (3)$$

The total Liouvillian is the sum of the spatial transport term $\mathcal{L}_{\text{trans}}$ and the local biological reaction term $\mathcal{L}_{\text{reac}}$.

We introduce the non-Abelian environmental gauge field $A_\mu(\mathbf{x})$, taking values in the Lie algebra of $SU(N)$. It is written in terms of the group generators T^a :

$$A_\mu(\mathbf{x}) = g \sum_a A_\mu^a(\mathbf{x}) T^a \quad (4)$$

where g is the coupling constant representing the mutation susceptibility. The standard spatial gradient ∂_μ for the infected multiplet is promoted to the gauge covariant derivative:

$$\mathcal{D}_\mu = \partial_\mu - A_\mu \quad (5)$$

In practical epidemiological applications, the non-Abelian gauge field $\mathbf{A}_\mu(\mathbf{x})$ is a measurable representation of spatially varying selective pressures. Biologically, this tensor field encodes geographic gradients in vector density (e.g., regional flea populations for *Yersinia pestis*), climatic temperature zones, host receptor distributions across ecotones, or localized anthropogenic interventions such as distinct agricultural boundaries. As a pathogen diffuses across these heterogeneous landscapes, the environment exerts a continuous mutational “friction” that selectively favors specific phenotypic conformations. Consequently, the covariant derivative $\mathcal{D}_\mu = \partial_\mu - \mathbf{A}_\mu$ formally couples geographic displacement to genomic rotation. This paradigm redefines phenotypic mutation: our model treats mutation as an active, advection-driven spatial transport process in place to be a time-dependent random event.

In quantum field theory, gauge interactions are typically introduced via the double covariant derivative $\mathcal{D}_\mu \mathcal{D}^\mu$. However, translating this minimal coupling directly to the Doi-Peliti formalism violates the conservation of probability in classical Markov processes, as $\langle |\mathcal{D}_\mu \mathcal{D}^\mu \neq 0$. To correctly map the biased spatial random walk (drift-diffusion) into our field theory while preserving the Markovian conservation of mass, the transport Liouvillian must take the Fokker-Planck form, utilizing an outer spatial divergence:

$$\mathcal{L}_{\text{trans}} = -D_I \int d^d x a_I^\dagger (\partial_\mu \mathcal{D}^\mu) a_I = -D_I \int d^d x a_I^\dagger \partial_\mu (\partial^\mu - A^\mu) a_I \quad (6)$$

The transport Liouvillian is constructed from the Laplacians:

$$\mathcal{L}_{\text{trans}} = -D_S \int d^d x a_S^\dagger \nabla^2 a_S - D_I \int d^d x \mathbf{a}_I^\dagger (\partial_\mu \mathcal{D}^\mu) \mathbf{a}_I \quad (7)$$

We model the infection ($S + I_i \xrightarrow{\beta} 2I_i$) and recovery ($I_i \xrightarrow{\gamma} \emptyset$). Using Doi’s rules, the transition $X \rightarrow Y$ contributes a term $\propto (a_{\text{in}}^\dagger - a_{\text{out}}^\dagger) a_{\text{in}}$ to the Liouvillian:

$$\mathcal{L}_{\text{reac}} = \int d^d x \left[\beta \sum_{i=1}^N (a_{I,i}^\dagger a_S^\dagger - a_{I,i}^{\dagger 2}) a_{I,i} a_S + \gamma \sum_{i=1}^N (a_{I,i}^\dagger - 1) a_{I,i} \right] \quad (8)$$

To transition to a classical field theory, we use coherent states. Operators are mapped to continuous fields ϕ , and creation operators are shifted using the Cole-Hopf-like transformation to isolate fluctuations:

$$a \rightarrow \phi, \quad a^\dagger \rightarrow 1 + \tilde{\phi} \quad (9)$$

Here, $\phi(\mathbf{x}, t)$ represents the density, and the response field $\tilde{\phi}(\mathbf{x}, t)$ represents the stochastic noise. The probability amplitude to go from an initial to a final state is given by the path integral $\int \mathcal{D}[\phi, \tilde{\phi}] e^{-S_{\text{eff}}}$, where the effective action is:

$$S_{\text{eff}} = \int dt d^d x \left[\tilde{\phi}_S \partial_t \phi_S + \tilde{\phi}_I^\dagger \partial_t \phi_I - \mathcal{H}(\phi, \tilde{\phi}) \right] \quad (10)$$

To find the Hamiltonian density \mathcal{H} , we normal-order \mathcal{L} and apply the shift:

$$\mathcal{H}_{\text{trans}} = D_S \tilde{\phi}_S \nabla^2 \phi_S + D_I \tilde{\phi}_I^\dagger \partial_\mu \mathcal{D}^\mu \phi_I \quad (11)$$

$$\mathcal{H}_{\text{reac}} = \beta \left(\tilde{\phi}_I^\dagger - \tilde{\phi}_S \mathbf{u}^T \right) \phi_I \phi_S - \gamma \tilde{\phi}_I^\dagger \phi_I + \mathcal{O}(\tilde{\phi}^2) \quad (12)$$

$\mathbf{u} = (1, 1, \dots, 1)^T$ is a vector used to sum over the contributions of all strains infecting a susceptible individual. Some remarks have to be done here:

- The Infected Field (ϕ_I): This field represents the pathogen, which has internal degrees of freedom (the N different strains). Therefore, it belongs to the fundamental representation of $SU(N)$. It is a column vector, and the generators T^a are non-zero $N \times N$ matrices (like the Pauli matrices for $SU(2)$). Thus, the gauge field actively rotates its components: $\mathcal{D}_\mu \phi_I = (\partial_\mu - \mathbf{A}_\mu) \phi_I$.
- The Susceptible Field (ϕ_S): This field represents the uninfected host population. It has no internal ‘‘strain’’ index; a person is simply susceptible. Mathematically, it belongs to the trivial representation (a gauge singlet) of the $SU(N)$ group.
- The gauge field A_μ in our model represents environmental pressures that force viral or bacterial mutation (e.g., ecological barriers, antiviral gradients, crossing species habitats).

We would use a covariant derivative for the susceptible population if we upgraded the biological assumptions of our model to give the hosts their own internal degrees of freedom that interact with the environment. For example, imagine a model with partial cross-immunity or different genetic phenotypes. If the host population consisted of different subtypes (e.g., S_A : naive to all strains, S_B : vaccinated against Strain 1 but susceptible to Strain 2), we would promote ϕ_S to a multiplet $\phi_S = (S_A, S_B)^T$. In that scenario, if the environment contained factors that changed host susceptibility (like a geographic gradient of a vaccine campaign or a vector-control chemical), we would introduce a second gauge field, say B_μ , acting on the S multiplet:

$$\mathcal{H}_{\text{trans}, S} = D_S \tilde{\phi}_S^\dagger \partial^\mu (\partial_\mu - B_\mu) \phi_S \quad (13)$$

III. THE MEAN-FIELD (CLASSICAL) LIMIT VIA SADDLE-POINT

The mean-field limit corresponds to the saddle-point approximation of the path integral, where the system follows the trajectory of stationary action. We demand that the functional variation of the action with respect to the response fields vanishes:

$$\frac{\delta S_{\text{eff}}}{\delta \tilde{\phi}_S} = 0, \quad \frac{\delta S_{\text{eff}}}{\delta \tilde{\phi}_I^\dagger} = \mathbf{0} \quad (14)$$

Evaluating these variations on the physical manifold where the stochastic noise vanishes ($\tilde{\phi}_S = 0, \tilde{\phi}_I = \mathbf{0}$) yields the classical equations of motion for the macroscopic densities $S(t) \equiv \phi_S$ and $\mathbf{I}(t) \equiv \phi_I$.

$$\partial_t S = D_S \nabla^2 S - \beta S (\mathbf{u} \cdot \mathbf{I}) \quad (15)$$

$$\partial_t \mathbf{I} = D_I \partial_\mu \mathcal{D}^\mu \mathbf{I} + \beta S \mathbf{I} - \gamma \mathbf{I} \quad (16)$$

To understand the phenomenological impact of the non-Abelian environment on the pathogen, we derive the macroscopic equation for the infected strains. Utilizing the Fokker-Planck transport operator to conserve classical probability [13, 14], and assuming the Lorentz/Coulomb gauge condition $\partial_\mu A^\mu = 0$, the equation for $I(t)$ becomes:

$$\partial_t \mathbf{I} = \underbrace{D_I \nabla^2 \mathbf{I}}_1 - \underbrace{2D_I A^\mu \partial_\mu \mathbf{I}}_2 + \underbrace{\beta S \mathbf{I} - \gamma \mathbf{I}}_3 \quad (17)$$

- $D_I \nabla^2 \mathbf{I}$ (**Standard Diffusion**): The conventional, isotropic spatial spreading of the pathogen populations.
- $-2D_I A^\mu \partial_\mu \mathbf{I}$ (**Mutational Advection**): It couples the spatial gradient of the pathogen density ($\partial_\mu \mathbf{I}$) with the environmental field (A^μ). To ensure the macroscopic population densities remain strictly real, the generators T^a are defined as Hermitian matrices (e.g., the Pauli matrix σ_3). Because A^μ is a non-diagonal matrix, this term generates an asymmetric flow. If a specific strain diffuses into a region with a strong gauge field, this term “rotates” the vector \mathbf{I} , actively mutating the pathogen into a different strain as a direct consequence of its spatial movement. If the Strain 1 population diffuses toward a specific zone (where the gradient $\partial_\mu I_1 \neq 0$), the environment forces a mutation, transforming part of that flux into Strain 2. Spatial movement generates active mutation.
- $\beta S \mathbf{I} - \gamma \mathbf{I}$ (**Biological Reaction**): The standard local, non-spatial SIR dynamics.

IV. TURING-HOPF INSTABILITY

The classic Turing Instability (or diffusion-driven instability) typically requires two interacting species with significantly different diffusion coefficients ($D_1 \neq D_2$) [15, 16]. However, in our non-Abelian Doi-Peliti model, both strains belong to the same $SU(2)$ multiplet and inherently share the same spatial diffusion coefficient D . The instability here is driven by the gauge field A_μ .

To illustrate the model, we shall assume that our gauge symmetry is given by $SU(2)$ with two different strains.

Defining the infected multiplet $\mathbf{I} = (I_1, I_2)^T$, we assume a constant environmental gauge field pointing in the x -direction: $\mathbf{A}_x = A\sigma^3$. We group the biological reaction terms into a single vector function $\mathbf{R}(\mathbf{I})$. The equation for $I(t)$ is given by:

$$\partial_t \mathbf{I} = D \partial_x^2 \mathbf{I} - 2DA_x \partial_x \mathbf{I} + \mathbf{R}(\mathbf{I}) \quad (18)$$

Because $\sigma^3 = \begin{pmatrix} 1 & 0 \\ 0 & -1 \end{pmatrix}$, the advection term splits asymmetrically:

- Strain 1 experiences a drift: $-2DA \partial_x I_1$
- Strain 2 experiences an opposite drift: $+2DA \partial_x I_2$

For spatial patterns to emerge, there must first be a uniform background state that is biologically stable [16, 17]. We define the Homogeneous Steady State (HSS) \mathbf{I}^* such that the biological reactions perfectly balance out:

$$\mathbf{R}(\mathbf{I}^*) = \mathbf{0} \quad (19)$$

If we completely removed the spatial dimensions ($D = 0$), small homogeneous perturbations $\delta \mathbf{I}(t)$ would evolve according to the Jacobian matrix \mathbf{J} evaluated at \mathbf{I}^* [18, 19]:

$$\partial_t \delta \mathbf{I} = \mathbf{J} \delta \mathbf{I}, \quad \text{where} \quad \mathbf{J} = \begin{pmatrix} J_{11} & J_{12} \\ J_{21} & J_{22} \end{pmatrix} \quad (20)$$

For this base state to be strictly stable against homogeneous biological fluctuations, the eigenvalues of \mathbf{J} must have negative real parts [18, 20]. This requires:

- Trace: $T_0 = J_{11} + J_{22} < 0$
- Determinant: $\Delta_0 = J_{11} J_{22} - J_{12} J_{21} > 0$

We now introduce small, spatially dependent perturbations with wave number k and temporal growth rate ω [16, 21]:

$$\delta\mathbf{I}(x, t) = \delta\mathbf{I}_0 e^{\omega t + ikx}$$

The linearized system becomes now an eigenvalue problem:

$$\omega\delta\mathbf{I} = \mathbf{M}(k)\delta\mathbf{I} \quad (21)$$

The characteristic matrix $\mathbf{M}(k)$ combines diffusion, gauge advection, and biology:

$$\mathbf{M}(k) = \mathbf{J} - Dk^2\mathbb{I} - 2iDkA\sigma^3 \quad (22)$$

Written out explicitly:

$$\mathbf{M}(k) = \begin{pmatrix} J_{11} - Dk^2 - 2iDkA & J_{12} \\ J_{21} & J_{22} - Dk^2 + 2iDkA \end{pmatrix} \quad (23)$$

to solve our initial equation, one needs to find the roots of the characteristic equation $\det(\mathbf{M}(k) - \omega\mathbb{I}) = 0$, which takes the form of a quadratic equation:

$$\omega^2 - T(k)\omega + \Delta(k) = 0 \quad (24)$$

We compute the spatial Trace $T(k)$ and Determinant $\Delta(k)$ of the matrix $\mathbf{M}(k)$:

$$T(k) = (J_{11} - Dk^2) + (J_{22} - Dk^2) = T_0 - 2Dk^2 \quad (25)$$

$$\Delta(k) = (J_{11} - Dk^2 - 2iDkA)(J_{22} - Dk^2 + 2iDkA) - J_{12}J_{21} \quad (26)$$

$$\Delta(k) = \Delta_R(k) + i\Delta_I(k) \quad (27)$$

where the trace $T(k)$ is real and always negative as $T_0 < 0$ (from our stable HSS condition) and $\Delta_R(k) = (J_{11} - Dk^2)(J_{22} - Dk^2) - J_{12}J_{21} + 4D^2k^2A^2$ and $\Delta_I(k) = 2DkA(J_{11} - J_{22})$.

For a spatial pattern to spontaneously form, the perturbations must grow. This means the complex eigenvalue $\omega = \alpha + i\beta$ must have a positive real part ($\alpha > 0$). Substitute $\omega = \alpha + i\beta$ into the characteristic equation:

$$(\alpha + i\beta)^2 - T(k)(\alpha + i\beta) + (\Delta_R + i\Delta_I) = 0 \quad (28)$$

$$\Rightarrow \begin{cases} \alpha^2 - \beta^2 - T(k)\alpha + \Delta_R = 0 \\ \beta(2\alpha - T(k)) = -\Delta_I \end{cases} \quad (29)$$

As we are interesting to get the condition on β when the instability start to grow, to get this β value, we set the growth rate to zero ($\alpha = 0$) and we get the following set of equations:

$$\beta^2 = \Delta_R \quad (30)$$

$$\beta = \Delta_I/T(k) \quad (31)$$

Substituting β from the second equation into the first yields the critical mathematical condition for the Turing-Hopf instability:

$$\left(\frac{\Delta_I}{T(k)}\right)^2 = \Delta_R \implies \Delta_I^2 = T(k)^2\Delta_R \quad (32)$$

For the instability to actively grow ($\alpha > 0$), the imaginary driving force must overcome the real damping terms. The rigorous condition is:

$$\Delta_I^2 > T(k)^2\Delta_R \quad (33)$$

Let us substitute our parameters back into the instability condition:

$$[2DkA(J_{11} - J_{22})]^2 > (T_0 - 2Dk^2)^2 [(J_{11} - Dk^2)(J_{22} - Dk^2) - J_{12}J_{21} + 4D^2k^2A^2] \quad (34)$$

To get formation of Hopf-Turing pattern, one needs:

- $J_{11} \neq J_{22}$: If the two strains have perfectly symmetric linear dynamics around the steady state ($J_{11} = J_{22}$), then $\Delta_I = 0$, the inequality fails, and no patterns form. The environment needs strains with differing inherent reaction rates to exploit.
- $A \neq 0$: If there is no mutational pressure, $\Delta_I = 0$, and standard uniform diffusion stabilizes the system.

Because the eigenvalue at the instability threshold is purely imaginary ($\omega = i\beta$), the resulting spatial pattern $\delta\mathbf{I} \propto e^{i\beta t + ikx}$ is not a stationary Turing spot. Instead, it is a traveling plane wave. As a conclusion, we have shown that an asymmetric environmental gauge field transforms a stable homogeneous mix of strains into continuous, self-sustaining traveling waves of mutation propagating across the geographic space.

V. DYNAMICAL EMERGENCE OF EPIDEMIOLOGICAL SAFE ZONES IN 2D

In the previous section, we established via linear stability analysis that a constant, non-Abelian environmental gauge field \mathbf{A}_μ can destabilize a homogeneous endemic state, driving a Turing-Hopf (Differential Flow) instability. We now demonstrate numerically that in a two-dimensional spatial domain, this gauge-driven instability spontaneously breaks spatial symmetry, generating continuous traveling waves. Crucially, we show that the destructive interference of these multiplet waves naturally generates propagating topological "safe zones"—regions completely devoid of the pathogen, formed without the need for static geographic barriers or prior immunological shields.

To observe the continuous formation of spatial patterns, we extend our biological reaction terms to an SIRS (Susceptible-Infected-Recovered-Susceptible) model. The inclusion of a finite immunity duration prevents the system from absorbing into a trivial extinct state, allowing the spatial instability to fully manifest.

Let the geographic space be a periodic 2D manifold with coordinates (x, y) . We define a constant, uniform environmental gauge field directed along the x -axis:

$$\mathbf{A} = (A_x, 0)\sigma^3 \quad (35)$$

where A_x is a constant representing a uniform ecological or mutational pressure across the domain, and σ^3 acts on the $SU(2)$ pathogen multiplet $\mathbf{I} = (I_A, I_B)^T$. Expanding the covariant Doi-Peliti effective action derived before, the governing macroscopic equations for the host densities (S, R) and the pathogen multiplet (I_A, I_B) are given by:

$$\partial_t S = D_S \nabla^2 S - \beta S(I_A + I_B) + \alpha R \quad (36)$$

$$\partial_t I_A = D_I \nabla^2 I_A - D_I A_x \partial_x I_A + \beta S I_A - \gamma I_A \quad (37)$$

$$\partial_t I_B = D_I \nabla^2 I_B + D_I A_x \partial_x I_B + \beta S I_B - \gamma I_B \quad (38)$$

$$\partial_t R = \gamma(I_A + I_B) - \alpha R \quad (39)$$

Here, α is the rate of immunity loss, β is the infection rate, and γ is the recovery rate. R represents the Recovered (or Immune) population.

To integrate this system, we employ a custom Explicit Finite Difference Time-Domain (FDTD) scheme over a discretized grid of $N_x \times N_y$ nodes.

- The standard Laplacian ∇^2 is approximated using a 5-point central difference stencil. The advective gradient terms ∂_x are evaluated using symmetric central differences to minimize numerical diffusion [22, 23].
- Our equations are integrated using an explicit Euler forward method. To guarantee numerical stability against the stiff reaction-diffusion dynamics, the time step Δt is strictly bounded by the Courant–Friedrichs–Lewy (CFL) condition for diffusion [24]:

$$\Delta t \leq \frac{(\Delta x)^2}{4 \max(D_S, D_I)}$$

- Periodic (toroidal) boundary conditions to eliminate edge effects are imposed to allow traveling waves to wrap continuously around the domain [25].
- The system is initialized near the theoretical homogeneous steady state (S^*, I_A^*, I_B^*, R^*) . To trigger the instability, we inject a microscopic, uniformly distributed white noise perturbation $\mathcal{O}(\epsilon)$ strictly into the pathogen fields $I_A(x, y, 0)$ and $I_B(x, y, 0)$ [25].

The system rapidly departs from the homogeneous state. Although I_A and I_B possess identical biological parameters (β, γ) , the σ^3 gauge field actively breaks their spatial degeneracy.

We can observe from the simulation the Emergence of Safe Zones. By observing the spatial distribution of the susceptible population $S(x, y, t)$, a geometric phenomenon emerges. The phase separation of the I_A and I_B waves leaves behind distinct, periodic spatial regions where the pathogen density is close to zero. These regions represent dynamically generated "safe zones". They do not exist because of static geography (as $\nabla \cdot \mathbf{A} = 0$) nor due to isolated quarantines. Instead, they are sustained by the destructive interference of the traveling waves.

Turing-Hopf Instability Driven by Uniform SU(2) Gauge Field

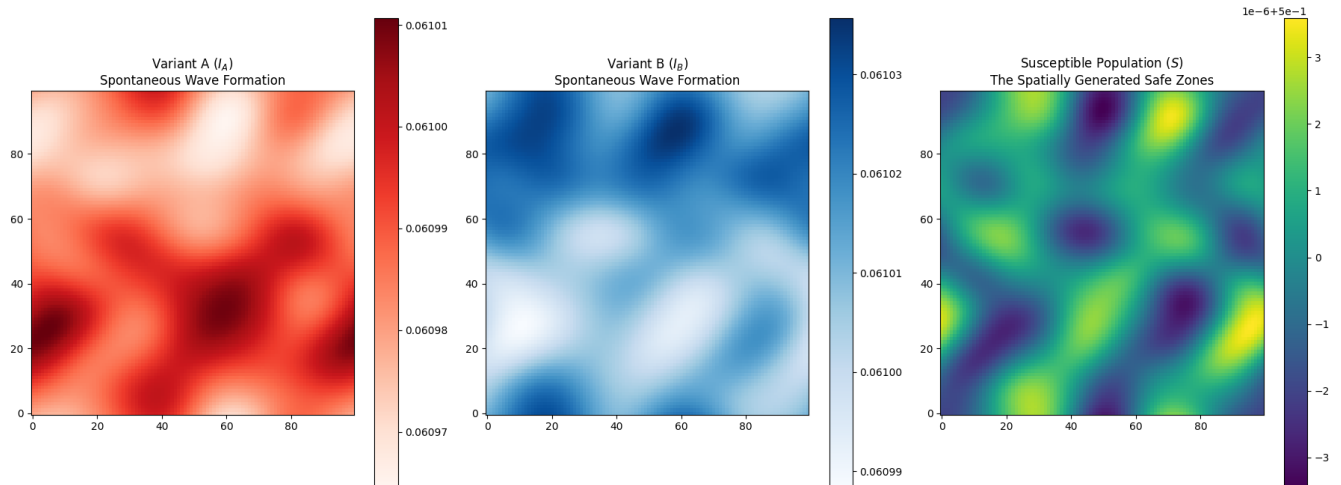


FIG. 1: a Turing-Hopf instability driven by a uniform SU(2) gauge field. It presents three heatmaps across a 2D space (x and y axes from 0 to 100) showing the spatial distribution and spontaneous pattern formation for three populations. Variant A (I_A) (left, in red tones) shows regions of spontaneous wave formation, with density varying between approximately 0.06097 and 0.06101. Variant B (I_B) (middle, in blue tones) similarly displays a wave-like pattern, complementary to Variant A, with density values ranging from about 0.06099 to 0.06103. The Susceptible Population (S) (right, in viridis tones) exhibits distinct regions of high and low susceptibility, varying narrowly around 0.5 (specifically from $0.5 - 3 \times 10^{-6}$ to $0.5 + 3 \times 10^{-6}$). The areas of higher susceptibility are labeled as spatially generated “safe zones,” emerging from the complex dynamics between the infected variants.

VI. PHENOMENOLOGICAL APPLICATION TO THE BLACK DEATH ANOMALY

Classical reaction-diffusion models of the Black Death (1347–1351) treat the pandemic as a homogeneous, isotropic wave of a single pathogen sweeping across Eurasia [1]. However, this classical approach fails to explain two major historical anomalies: the sudden genetic radiation of the pathogen [3, 4], and the existence of vast, untouched geographic “safe zones” (such as Milan, the Basque Country, and parts of Poland) surrounded by total demographic collapse [5, 26].

A. Static Gauge Barriers: Geography and Quarantine

While comprehensive space-time geostatistical models, such as those developed by Christakos et al. [2, 27], accurately map the macroscopic velocity and duration of the Black Death’s advance [28], they must often treat spared regions as isolated data anomalies or impose them via strict, ad-hoc boundary conditions. In our model, the sparing of specific regions, such as the Pyrenees mountains and the city-state of Milan, can be explained by sharp local gradients in the static geographic gauge field, \mathbf{A}_{geo} .

- **Topographical Advection:** In the case of the Basque Country, the Pyrenees represents a strong advective headwind ($-2D_I \mathbf{A}_{\text{geo}} \cdot \nabla \mathbf{I}$). The differential flow instability naturally channels the traveling wave of the infection along paths of least covariant resistance physically bypassing the isolated mountain populations.
- **Anthropogenic Friction:** Milan famously enacted a ruthless, state-enforced quarantine.

B. Poland and Bohemia Black death anomaly

Perhaps the most enigmatic safe zones of the Black Death were regions like Poland and Bohemia, which lacked extreme geographic barriers or strict Milanese-style quarantines, but suffered significantly lower mortality [5].

1. The $SU(N)$ "Big Bang" of *Yersinia pestis*

Modern paleogenomic analysis of ancient DNA extracted from 14th-century victims reveals that the Black Death was not caused by a single static pathogen [4]. Instead, it was associated with a massive evolutionary radiation event known as the plague "Big Bang," where a single ancestral strain rapidly diverged into at least four distinct genetic lineages [3].

In our formalism, this is modeled by upgrading the pathogen field to an $SU(N)$ multiplet, where $N \geq 4$. Due to the lack of information on these different strain, we shall apply our model in the limit of $N \rightarrow \infty$.

2. The Large- N Continuum and 't Hooft Scaling

In the discrete model, the total pathogen load is the sum of N distinct variants. In the limit $N \rightarrow \infty$ [11], the discrete mutational space transitions into a continuous angular spectrum $\theta \in [0, 2\pi)$. The discrete $SU(N)$ advection vectors simultaneously map onto a continuous, angle-dependent gauge vector field $\mathbf{v}(\theta)$, dictating the spatial transport of each specific strain:

$$\mathbf{v}(\theta) = A_{\max}(\cos \theta \hat{\mathbf{e}}_x + \sin \theta \hat{\mathbf{e}}_y) \quad (40)$$

In the discrete model, the total pathogen load is the sum of N distinct strains. In the 't Hooft continuum limit ($N \rightarrow \infty$), the discrete mutational space becomes a continuous angular spectrum $\theta \in [0, 2\pi)$. We define the macroscopic mean-field pathogen density, $\Phi(\mathbf{r}, t)$, by integrating the continuous pathogen distribution $I(\mathbf{r}, \theta, t)$ over all possible advection angles:

The spatiotemporal evolution of this continuous pathogen spectrum is governed by the following integro-differential equation [29, 30]:

$$\frac{\partial I(\mathbf{r}, \theta, t)}{\partial t} = D_I \nabla^2 I(\mathbf{r}, \theta, t) - \mathbf{v}(\theta) \cdot \nabla I(\mathbf{r}, \theta, t) + \beta S(\mathbf{r}, t) I(\mathbf{r}, \theta, t) - \gamma I(\mathbf{r}, \theta, t) \quad (41)$$

To prevent the total interaction energy from diverging as the number of variants approaches infinity, the system must undergo a scaling analogous to the 't Hooft limit in quantum chromodynamics [11]. We define the macroscopic mean-field pathogen load, $\Phi(\mathbf{r}, t)$, by integrating over the entire continuous phase space and normalizing by 2π [31]:

$$\Phi(\mathbf{r}, t) = \frac{1}{2\pi} \int_0^{2\pi} I(\mathbf{r}, \theta, t) d\theta \quad (42)$$

This mean-field tensor couples back to the host population dynamics, ensuring the transmission pressure remains bounded. The corresponding equations for the Susceptible (S) and Removed (R) populations become:

$$\frac{\partial S(\mathbf{r}, t)}{\partial t} = D_S \nabla^2 S(\mathbf{r}, t) - \beta S(\mathbf{r}, t) \Phi(\mathbf{r}, t) + \alpha R(\mathbf{r}, t) \quad (43)$$

$$\frac{\partial R(\mathbf{r}, t)}{\partial t} = \gamma \Phi(\mathbf{r}, t) - \alpha R(\mathbf{r}, t) \quad (44)$$

3. The Plane Wave Ansatz in the Differential Flow Induced Instability (DIFII) regime

In the Differential Flow Induced Instability regime, the invasion fronts of the pathogen propagate as macroscopic waves driven by the gauge field $\mathbf{v}(\theta)$ [10]. Near the central collision region (the geographical center of the outbreak havens, \mathbf{r}_c), we approximate these incoming fronts as a superposition of intersecting plane waves [32]. For a specific variant defined by angle θ , its wave vector \mathbf{k}_θ aligns with its advective transport:

$$\mathbf{k}_\theta = k(\cos \theta \hat{\mathbf{e}}_x + \sin \theta \hat{\mathbf{e}}_y) \quad (45)$$

where k is the wave number (spatial frequency) determined by the diffusion-advection parameters. As we are interested by the stationary spatial interference pattern, we drop the temporal oscillatory term $e^{-i\omega t}$. The complex spatial amplitude of a specific strain radiating toward the collision center \mathbf{r}_c is therefore given by the ansatz:

$$I(\mathbf{r}, \theta) = I_0 e^{i\mathbf{k}_\theta \cdot (\mathbf{r} - \mathbf{r}_c)} \quad (46)$$

4. Analytical Integration and Bessel Topology

Substituting this plane wave ansatz into our mean-field integral yields:

$$\Phi(\mathbf{r}) = \frac{I_0}{2\pi} \int_0^{2\pi} e^{i\mathbf{k}_\theta \cdot (\mathbf{r} - \mathbf{r}_c)} d\theta \quad (47)$$

Defining $\mathbf{R} = \mathbf{r} - \mathbf{r}_c$ as the radial distance from the center of Poland and using polar coordinates:

$$\mathbf{R} = R(\cos \phi \hat{\mathbf{e}}_x + \sin \phi \hat{\mathbf{e}}_y) \quad (48)$$

Using the definition of k_θ and R as given above, $\Phi(r)$ can be written as:

$$\Phi(\mathbf{r}) = \frac{I_0}{2\pi} \int_0^{2\pi} e^{ikR \cos(\theta - \phi)} d\theta \quad (49)$$

Using the standard Bessel relation $e^{iz \cos \alpha} = \sum_{n=-\infty}^{\infty} i^n J_n(z) e^{in\alpha}$ where $J_n(z)$ is the n -th order Bessel function of the first kind. Using this relation and integrating on θ , one gets

$$\Phi(\mathbf{r}) = \frac{I_0}{2\pi} (i^0 J_0(kR) e^0(2\pi)) \quad (50)$$

$$\Phi(\mathbf{r}) = I_0 J_0(k|\mathbf{r} - \mathbf{r}_c|) \quad (51)$$

Although paleogenomic data explicitly resolves only a small finite number of major lineages ($N \geq 4$) during the plague polytomy. We have to note that

- While historical paleogenomics explicitly identifies at least four major branching lineages ($N \geq 4$) during the plague “Big Bang,” these represent most probably only the dominant, surviving macroscopic clusters within a much denser, near-continuous quasispecies spectrum.
- Mathematically, the central interference node generated by a symmetric discrete superposition of a few ($N \geq 4$) intersecting plane waves is already dominated by the zeroth-order Bessel function $J_0(kr)$ near the origin.

Consequently, transitioning to the $N \rightarrow \infty$ continuous angular limit $\theta \in [0, 2\pi)$ is physically justified, as it effectively coarse-grains over the unresolved microscopic variants to capture the mean-field mutational transport and for $N \geq 4$, the zeroth order of Bessel function is given an good approximation of the diffraction wave pattern close to the origin.

5. The Geometry of the Safe Zone

The Susceptible population $S(\mathbf{r})$ survives in the topological “voids” where the macroscopic pathogen waves destructively interfere. Thus, the spatial distribution of the surviving host density is proportional to the squared norm of the mean-field interference pattern:

$$S(\mathbf{r}) \propto |\Phi(\mathbf{r})|^2 \quad (52)$$

Substituting our solution for $\Phi(\mathbf{r})$ yields the final analytical result:

$$S(\mathbf{r}) \propto |I_0 J_0(k|\mathbf{r} - \mathbf{r}_c|)|^2 \quad (53)$$

6. Fixing the Spatial Wave Number k and Geographic Boundary Matching

The topological structure of the macroscopic safe zone is governed by the spatial wave number k , which dictates the frequency of the diffraction fringes. In this gauge model, k is not an arbitrary fitting parameter, but is determined by the intrinsic physical scales of the Differential Flow Induced Instability.

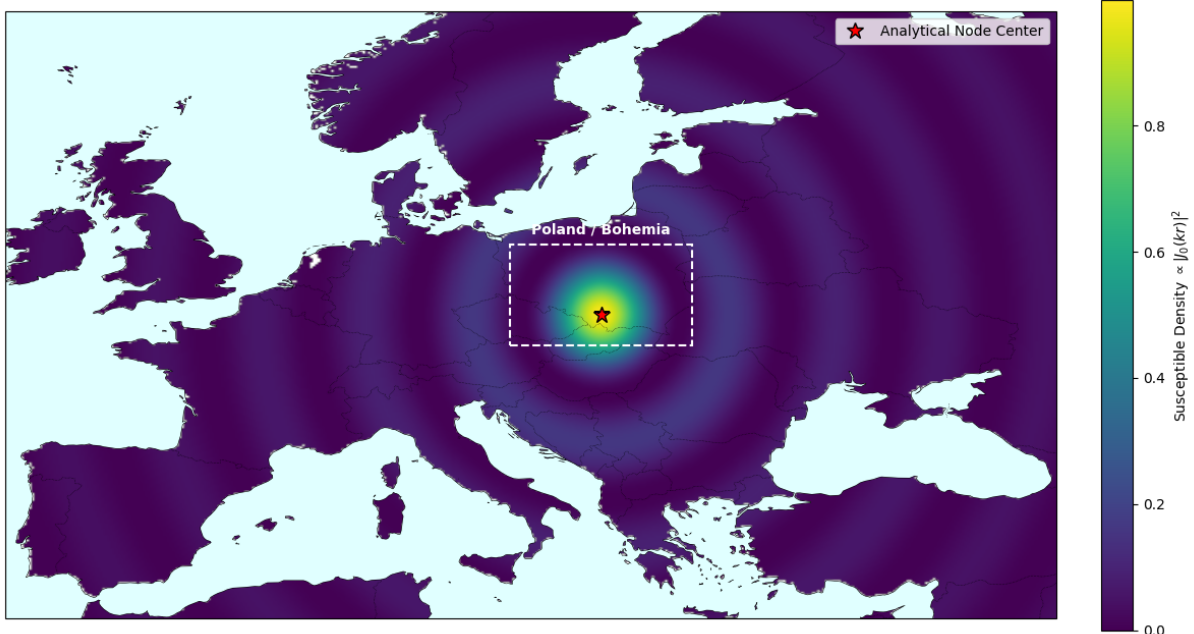
Analytical Large- N Limit: J_0 Bessel Intensity over Southern Poland

FIG. 2: This map visualizes the precise, steady-state spatial topology of host survival probability, derived analytically in the preceding section for the infinitely diverse mutational limit. The vibrant colormap represents the normalized intensity—or squared macroscopic amplitude—of the zeroth-order Bessel function of the first kind: $S(\mathbf{r}) \propto |J_0(k|\mathbf{r} - \mathbf{r}_c)|^2$. The concentric diffraction pattern is explicitly centered on the historical haven coordinates of Southern Poland (\mathbf{r}_c , marked by a red star). Physically, this translates to an undepleted host population that is topologically protected from infection. Deep purple represents the concentric diffraction ‘dead zone’ ripples.

Theoretically, the dominant spatial mode characterizing the interference pattern corresponds to the critical wave number, k_c , that maximizes the real part of the temporal growth rate in the linear dispersion relation derived in Section IV [21]:

$$\left. \frac{\partial \text{Re}(\omega(k))}{\partial k} \right|_{k=k_c} = 0 \quad (54)$$

This condition links the macroscopic geographic width of the safe zone to the microscopic biological parameters: the pathogen diffusion tensor D_I , the environmental gauge coupling A , and the kinetic reaction rates β and γ [16].

As we don’t have access to these parameters in the case of the Black death epidemics, we shall fix the k_c parameter to the historical extension of the observed “safe” zone in Poland, R_{safe} .

$$kR_{\text{safe}} = 2.4048 \implies k = \frac{2.4048}{R_{\text{safe}}} \quad (55)$$

where 2.4048 is the first Bessel root.

VII. CONCLUSION

In this work, we have demonstrated that embedding pathogen dynamics within a non-Abelian gauge space resolves the spatial anomalies of multi-strain pandemics. By utilizing the Doi-Peliti formalism, we mapped the stochastic biological interactions of mutating pathogens into a covariant classical field theory. We proved that spatial variations in environmental pressures—represented as the gauge field \mathbf{A}_μ —act as an asymmetric advective force that breaks the spatial degeneracy of the strains, driving a Turing-Hopf instability.

Crucially, our results reveal that historical epidemiological safe zones, such as 14th-century Poland and Bohemia, do not require the assumption of perfectly sealed borders or impenetrable geographic fortresses. Instead, these regions

emerge deterministically as topological “voids” sustained by the macroscopic destructive interference of colliding pathogen waves. In the ’t Hooft limit, the infinite mutational spectrum perfectly smooths these safe zones into isotropic, J_0 Bessel-governed diffraction nodes. Beyond the historical application to the Black Death, our gauge model is a new method that can be used, from modeling antimicrobial resistance gradients in hospital infrastructure to mapping the trajectory of zoonotic spillovers across wild-urban ecotones.

Acknowledgments

We acknowledge financial support from SECIHTI and SNII (México).

-
- [1] J. V. Noble, *Nature* **250**, 726 (1974).
 - [2] G. Christakos, R. A. Olea, M. L. Serre, H.-L. Yu, and L.-L. Wang, *Interdisciplinary Public Health Reasoning and Epidemic Modelling: The Case of Black Death* (Springer-Verlag, Berlin, Heidelberg, 2005).
 - [3] Y. Cui, C. Yu, Y. Yan, D. Li, Y. Li, T. Jombart, L. A. Weinert, Z. Wang, Z. Guo, L. Xu, *et al.*, *Proceedings of the National Academy of Sciences* **110**, 577 (2013).
 - [4] M. A. Spyrou, M. Keller, R. I. Tukhbatova, C. L. Scheib, E. A. Nelson, A. Andrades Valtueña, G. Neumann, D. Walker, A. Alterauge, N. Carty, *et al.*, *Nature Communications* **10**, 4470 (2019).
 - [5] A. Izdebski, P. Guzowski, R. Poniak, L. Masci, J. Palli, C. Vignola, M. Bauch, C. Coccozza, R. Fernandes, F. C. Ljungqvist, *et al.*, *Nature Ecology & Evolution* **6**, 297 (2022).
 - [6] M. Doi, *Journal of Physics A: Mathematical and General* **9**, 1465 (1976).
 - [7] L. Peliti, *Journal de Physique* **46**, 1469 (1985).
 - [8] U. C. Täuber, M. Howard, and B. P. Vollmayr-Lee, *Journal of Physics A: Mathematical and General* **38**, R79 (2005).
 - [9] U. C. Täuber, *Critical Dynamics: A Field Theory Approach to Equilibrium and Non-Equilibrium Scaling Behavior* (Cambridge University Press, 2014).
 - [10] A. B. Rovinsky and M. Menzinger, *Physical Review Letters* **69**, 1193 (1992).
 - [11] G. ’t Hooft, *Nuclear Physics B* **72**, 461 (1974).
 - [12] J. d. J. Bernal-Alvarado and D. Delepine, arXiv preprint arXiv:2602.13913 10.48550/arXiv.2602.13913 (2026).
 - [13] H. Risken, *The Fokker-Planck Equation: Methods of Solution and Applications*, 2nd ed. (Springer-Verlag, Berlin, Heidelberg, 1989).
 - [14] A. Lefèvre and G. Biroli, *Journal of Statistical Mechanics: Theory and Experiment* **2007**, P07024 (2007).
 - [15] A. M. Turing, *Philosophical Transactions of the Royal Society of London. Series B, Biological Sciences* **237**, 37 (1952).
 - [16] J. D. Murray, *Mathematical Biology II: Spatial Models and Biomedical Applications*, 3rd ed. (Springer-Verlag, New York, 2003).
 - [17] L. A. Segel and J. L. Jackson, *Journal of Theoretical Biology* **37**, 545 (1972).
 - [18] S. H. Strogatz, *Nonlinear Dynamics and Chaos: With Applications to Physics, Biology, Chemistry, and Engineering*, 2nd ed. (CRC Press, Boca Raton, 2015).
 - [19] M. J. Keeling and P. Rohani, *Modeling Infectious Diseases in Humans and Animals* (Princeton University Press, Princeton, 2008).
 - [20] L. Edelstein-Keshet, *Mathematical Models in Biology* (Society for Industrial and Applied Mathematics (SIAM), Philadelphia, 2005).
 - [21] M. C. Cross and P. C. Hohenberg, *Reviews of Modern Physics* **65**, 851 (1993).
 - [22] R. J. LeVeque, *Finite Difference Methods for Ordinary and Partial Differential Equations: Steady-State and Time-Dependent Problems* (Society for Industrial and Applied Mathematics (SIAM), Philadelphia, 2007).
 - [23] J. H. Ferziger and M. Perić, *Computational Methods for Fluid Dynamics*, 3rd ed. (Springer-Verlag, Berlin, Heidelberg, 2002).
 - [24] J. C. Strikwerda, *Finite Difference Schemes and Partial Differential Equations*, 2nd ed. (Society for Industrial and Applied Mathematics (SIAM), Philadelphia, 2004).
 - [25] M. C. Cross and H. Greenside, *Pattern Formation and Dynamics in Nonequilibrium Systems* (Cambridge University Press, Cambridge, 2009).
 - [26] O. J. Benedictow, *The Black Death, 1346-1353: The Complete History* (Boydell Press, Woodbridge, UK, 2004).
 - [27] G. Christakos, R. Olea, and H.-L. Yu, *Public Health* **121**, 700 (2007).
 - [28] R. A. Olea and G. Christakos, *Human Biology* **77**, 291 (2005).
 - [29] B. Perthame, *Transport Equations in Biology*, *Frontiers in Mathematics* (Birkhäuser Basel, 2007).
 - [30] M. C. Marchetti, J. F. Joanny, S. Ramaswamy, T. B. Liverpool, J. Prost, M. Rao, and R. A. Simha, *Reviews of Modern Physics* **85**, 1143 (2013).
 - [31] Y. Kuramoto, *Chemical Oscillations, Waves, and Turbulence* (Springer-Verlag, Berlin, Heidelberg, 1984).
 - [32] R. B. Hoyle, *Pattern Formation: An Introduction to Methods* (Cambridge University Press, Cambridge, 2006).